

NUMERICAL ANALYSIS OF THE WIRE-MESHED NET ANCHORAGED

¹RISKI PURWANA PUTRA, ²ALI LIMAM, ³DATA IRANATA

¹BPPW Kalimantan Utara Ministry of Public Works and Housing Tanjung Selor, Indonesia.

²Dept. Genie Civil et Urbanisme LGCIE, INSA de Lyon Lyon, France.

³Department of Civil Engineering, ITS Surabaya, Indonesia.

e-mail : riskiputra@pu.go.id, ali.limam@insa-lyon.fr, data.iranata@ce.its.ac.id,

ABSTRACT

The rockfall hazard in areas such as mountainous regions, quarries and mines needs to be well managed. This is essential in order to avoid fatalities, damage to infrastructure and production losses. Preventing all rockfall events is almost impossible, but the installation of rockfall protection systems is a common and effective way to control the hazard. The installation of wire-meshed net anchored is a possible solution to prevent slippage of landslide of the surface layers. This paper will be focused on the study of numerical modeling, using finite element analysis software, ABAQUS, of double-twisted hexagonal wire-meshed net anchored which has been developed by the French-based company, GTS. The objective is to analyze several configurations and performances of wire-meshed nets, cables. As final result, we will comparing between the experiment and numerical modeling analysis.

Keywords : Wire mesh net; cable net; finite element analysis.

1. INTRODUCTION

Metallic wire meshes are a key component of various types of structural protection measures against rockfall such as embankments, catch fences and draperies. Commonly used wire meshes include chain link and double-twisted hexagonal meshes [4]. Figure 1 shows two applications of a double-twisted hexagonal wire mesh as part of a rockfall protection system. The wire mesh, installed in a complex rockfall barrier structure. Various approaches for modelling rockfall protection systems with steel wire meshes have been proposed in the literature [3]. The finite element method (FEM) is the most common and can be used to simulate the impact of falling rocks or landslide slippage against protection systems and to investigate their energy absorption capacity [1]. The FEM is well established for dynamic modelling of continuum problems with non-linear geometrics, complex mechanical behavior, and various contact conditions [7].

2. STUDY REFERENCES

A. Systems of protection

There is a large panel of techniques to fight against the impact of a rockfall. Typically, rockfall events are mitigated in one of two ways: either by passive mitigation or active mitigation. Passive mitigation is where only the effects of the rockfall event are mitigated and are generally employed in the deposition or run-out zones, such as through the use of drape

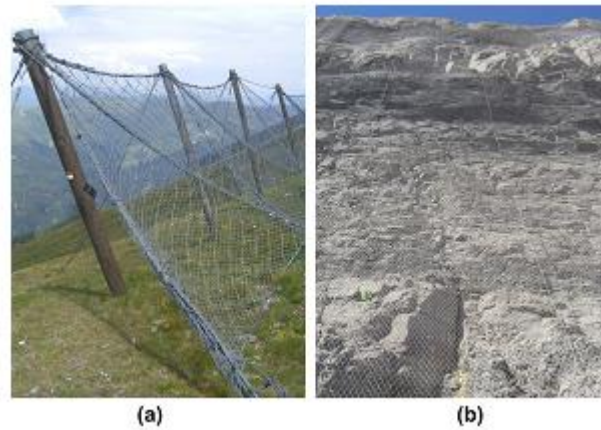


Figure 1. Applications of double-twisted hexagonal meshes in rockfall protection: (a) rockfall catch fence and (b) simple mesh drapery system. (Thoeni et al, 2012).

nets (Figure. 1(a)), rockfall catchment fences, diversion dams, etc. The rockfall still takes place but an attempt is made to control the outcome. In contrast, active mitigation is carried out in the initiation zone and prevents the rockfall event from ever occurring. Some examples of these measures are rock bolting, slope retention systems (Fig. 1(b)), shotcrete, etc. Other active measures might be by changing the geographic or climatic characteristics in the initiation zone, e.g. altering slope geometry, dewatering the slope, revegetation, etc.

B. Wire Mesh Characteristics

As pointed out by Bertrand [5], hexagonal wire meshes are woven systems. They are made by twisting continuous pairs of steel wires to form hexagonal-shaped openings as shown in Fig. 2. The hexagonal honeycomb-like structure increases the macroscopic strength of the wire mesh and the double twists ensure that failure of a single wire does not compromise the panel. The lateral sides of the mesh are mechanically selvaged in parallel to the double-twists with a slightly thicker wire which is of the same material. This work considers the GTS double-twisted hexagonal wire mesh of type 60x80 and 100x120 with a wire diameter of 2.7mm. The diameter of the selvedge wire is 3.4 mm, and the characteristics and dimensions of the mesh which are relevant to this research are summarized in Table 1.

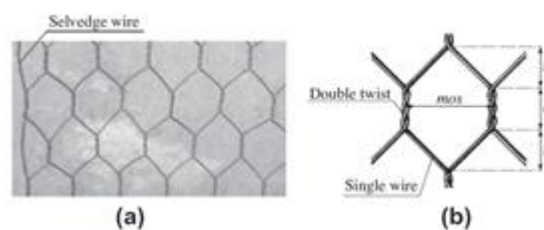


Figure 2. Characteristics of a double twisted hexagonal mesh: (a) close-up view of a double-twisted hexagonal wire mesh (b) definition of the size of a hexagon. (Thoeni, 2012).

Table 1 Characteristics of Wire Mesh.

Characteristics	GTS 60x80	GTS 100x120
Length ($a+2b$)	80	120
Width (mos)	60	100
Wire Diameter	2.7 mm	2.7 mm ²
Wire Resistance	500 N/mm ²	500 N/mm ²
Mass per unit area	1.4 kg/m ²	1.4 kg/mm ²

A series of tensile tests were performed by Thoeni et al. on single wires produced by Maccaferri of diameter of 2.7 mm and 3.4 mm and on double-twists of a wire diameter of 2.7 mm. The length of the samples was between 120 and 150 mm and, during the tests, the wire ends were clamped within the testing device. Thus, tension was applied to an effective length ranging from 40 to 50 mm. Fig. 3 summarises the force-displacement curves of all the wire tests. The stress-strain curves for the single wires and the double-twists are shown in Fig. 4a and b respectively.

C. Cable characteristics

The cable is the basic element of the structure, its primary function in this work is to transmit the forces throughout the change process of wire mesh [2].

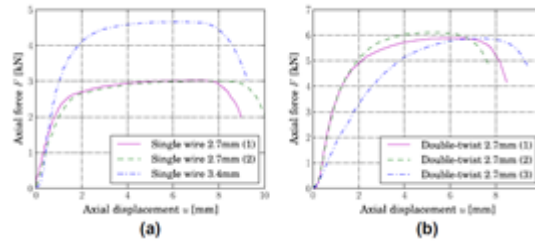


Figure 3. Experimental force-displacement curves of the tested: (a) single wires and (b) double-twist. (Thoeni, 2012).

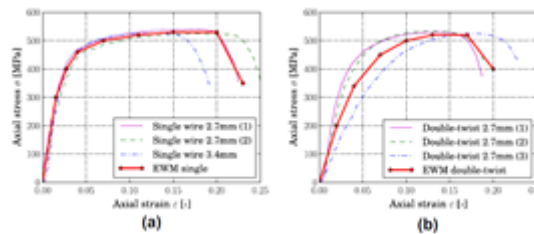


Figure 4. Stress-strain curves for:(a) single wires and (b) double-twist. (Thoeni, 2012).

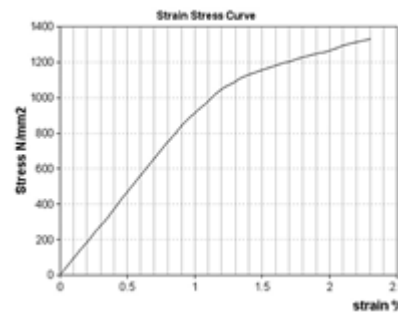


Figure 5. Characteristic stress-strain curves of 8 mm nominal diameter cable (Fresno, 2012).

D. Numerical simulation

The solution for the simulation of the net tests implies the simultaneous study of two non-linearities: (1) material non-linearity (plastic behaviour in this case) and (2) geometric non-linearity of large net displacements.

• Plasticity

Plastic behavior of solids is characterized by a non-unique stress-strain relationship as opposed to that of non-linear elasticity. Indeed, one definition of plasticity may be the presence of unrecoverable strains on load removal. Many materials show an ideal plastic behavior in which a limiting yield stress, σ_y , exists at which the strains are indeterminated. It is generally postulated, as an experimental fact, that yield can occur only if the stresses σ satisfy the general yield criterion [8]:

$$F(\sigma, \kappa) = 0 \quad (1)$$

Where κ is a ‘hardening’ parameter. This yield condition can be visualized as a surface in n-dimensional space of stress with the position of the surface F (yield surface) dependent on the instantaneous value of the state parameter κ .

- Large displacements

In many problems it has been implicitly assumed that both displacements and strains developed in the structure are small. In practical terms, this means that the geometry of the elements remains basically unchanged during the loading process and that first-order, infinitesimal, linear strain approximations can be used. In many cases, very large displacements may occur without causing large strains. Typical in this context is the classical problem of the ‘elastica’ of which an example is a watch spring.

Whether the displacements (or strains) are large or small, equilibrium conditions between internal and external ‘forces’ have to be satisfied. Thus, if the displacements are prescribed in the usual manner by a finite number of nodal parameters \vec{a} , we can obtain the necessary equilibrium equations using the virtual work principle [11]:

$$\Psi(\vec{a}) = \int_V \bar{B}^T \vec{\sigma} dV - \vec{f} = 0 \quad (2)$$

where Ψ once again represents the sum of external and internal generalized forces, and in which B is defined from the strain definition as :

$$d\vec{\varepsilon} = \bar{B} d\vec{a} \quad (3)$$

The bar suffix has now been added so that, if displacements are large, the strains depend on displacement non-linearly, and the matrix B is now dependent on \vec{a} . We see that it can be conveniently rewritten [10]:

$$\bar{B} = B_0 + B_L(\vec{a}) \quad (4)$$

In which B_0 is the same matrix as in linear infinitesimal strain analysis and only B_L depends on the displacement. In general, B_L will be found to be a linear function of such displacements. Clearly the solution of Eq. (2) will have to be approached iteratively. Newton-type iteration can once more be applied precisely in order to solve the final non-linear problem.

E. Loadings

- Quasi-static Loading

The quasi-static load is the load that is applied slowly to the structure, it also deforms very slowly. That is the type of loading used in the numerical modeling. In solid mechanics, quasi-static loading refers to loading where inertial effects are negligible. In other words time and inertial mass are irrelevant [2].

3. INVESTIGATION OF THE TEST

A. Introduction

These tests were carried out by Francis Jeannin in collaboration with wire mesh producer, GTS, allowed the author to remake in numerical modeling. The experimental test consists of 5 configurations of wire mesh net. Fig.5. is a sort of configuration sketch that has been tested experimentally.

B. Description of Testing Instruments

The tray component as shown in Fig.6. consists of steel web profile fixed together at each corner of a bar and bolted through the two dimensions. Inside this tray, there is a water filled tanks. These 3x3 meter tanks will apply a uniform stress on the wire mesh net, under pressure the hydraulic cylinders.

The cylinder exerts a force F through an anchor plate, width l . It applies a pressure $f = F/l2$ on the wire mesh.

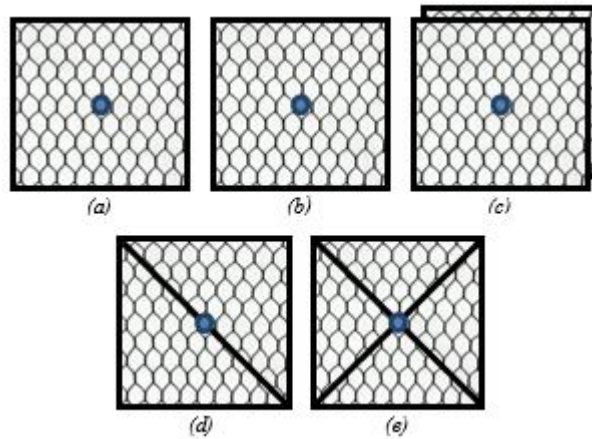


Figure. 6. (a) Wire mesh 60x80, (b) Wire mesh 100x120, (c) Double sheet wire mesh, (d) Wire mesh with 1 cable, (e) Wire mesh with 2 cables.

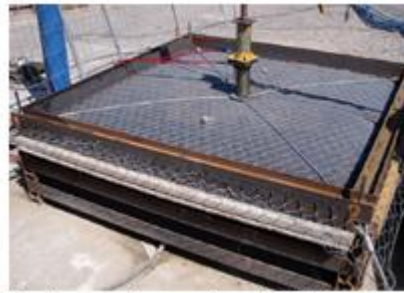


Figure. 7. Installation of wire mesh with 2 Cables (Jeannin, 2013).

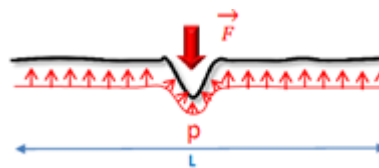


Fig.8. Schema of the Applied Stress (Jeannin, 2013).

Under the pressure of the plate, the wire mesh deformed locally and the water tank then exerts a uniform pressure over the entire wire mesh surface. So we have the following relationship : $p \cdot L2 = f \cdot l2$

Where L is a length or width of the wire mesh which is 3 meters.

C. Experimental Results

After the experimental test was performed, we obtained a list of resistance capacity for each configuration of the wire mesh net:

TABEL II. Experimental Resistant Capacity

Configuration	Averaged Resistance Capacity (kN)
Wire mesh 60x80	27
Wire mesh 100x120	24
Double sheet wire mesh	42
Wire mesh with 1 cable	40
Wire mesh with 2 cables	160

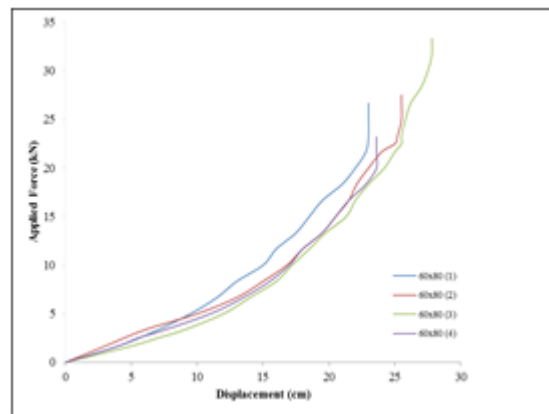


Figure.9. Loading Curve of Wire Mesh 60x80 (Jeannin, 2013).

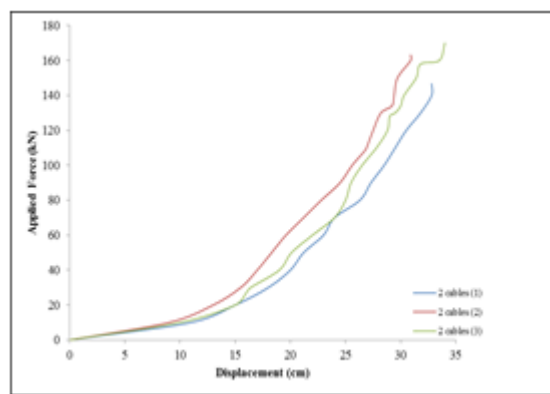


Figure.10. Loading Curve of Wire Mesh 100x120 with 2 cables (Jeannin, 2013).

4. NUMERICAL MODELING

The numerical model of the structure is presented to demonstrate as simple, and as realistic as possible. Not all elements of the experimental properties, such as water tank, hydraulic cylinder, are modeled in this case. For simplicity, we can discuss the numerical modeling steps as below:

A. Wire mesh net

The net is modeled as a double-twist hexagonal, which is composed of two lateral sides of each twisted wire. The position of the loads in the nodes can be deduced starting as shown in Figure.11. All edges of the surface of net screens as shown in Fig.12. are considered as triple supports, three movements are blocked and the three rotations are free



Figure.11. Distribution of loads in wire mesh net nodes.

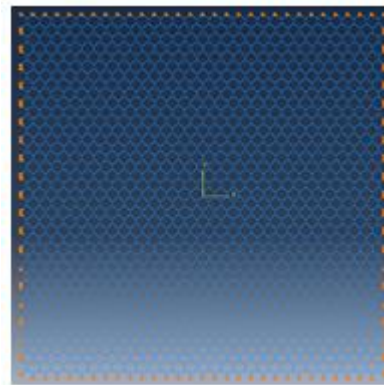


Figure.12. Boundary Condition of Wire Mesh Net.

The applied force to each configuration of the wire mesh net is based on maximum force which has been noted on the experimental test.

TABEL III. Experimental Resistant Capacity

Configuration	Applied Force (kN)
Wire mesh 60x80	33.3
Wire mesh 100x120	29.2
Double sheet wire mesh	43.1
Wire mesh with 1 cable	42.7
Wire mesh with 2 cables	170.3

(Jeamin, 2013)

To exert a force, the hydraulic cylinder is used to transmit a force to the anchor plate surface, is equal to 20cmx20cm. In this case, we can just exert the force directly to the nodes of wire mesh net corresponds to the anchor plate surface, as shown in Fig.11.

B. Wire rope cable

The cable is used in this numerical analysis is a type of steel wire rope cable with a diameter of 16 mm, and it has Young's modulus of 90000 MPa and the density of 4.87×10^{-9} ton/m³.

C. Membrane

The water tank in the tray is designed to provide pressure on the surface of the net. To simplify in the Finite Element Method (FEM), we can install a membrane element to apply the vertical pressure pushing the net surface. A membrane may be composed of an elastic material such as rubber.

TABEL IV. Membrane Material Properties

Membrane density	1000 kg/m ³
Membrane Young's modulus	3×10^8 N/mm ²
Membrane Poisson's ratio	0.35
Thickness	6.25 mm

(Potula, 2012)



Figure.13. Numerical model assembly of wire mesh



Figure.14. Loading Scheme: (a) 1st step: Pressure on membrane,
(b) 2nd step: Concentrated Force on mesh nodes.

D. Contact Modeling

In each experimental structure of a mesh configuration, there are three major components to build as shown in Fig.13, they are: wire mesh itself, membrane, and cable. To assembly in ABAQUS, we must manage the contact between each of them. In this case, the author choose the tangential behavior without friction. And for normal behavior, the relationship between pressure and over-closure, the author modeled in hard contact (Hard Contact).

E. Loading Scheme

The forces indicated above are given at the nodes which has been discussed previously. In numerical analysis, there are two steps of loading force. As shown in Fig. 14, the first step, a pressure force pushes the membrane towards the upper which equal the maximum force divided by the membrane section area. The second step, the maximum force pushes the net downwards. This calculations use the Dynamic method ABAQUS/Explicit.

5. RESULT AND DISCUSSION

A. Deformed Shape

After modeling wire mesh net in ABAQUS, the overall shapes of the deformed wire mesh net are obtained as shown in Fig.15. and compared with experimental results. This comparison shows a good accordance between the numerical results and the experimental results.

B. Load-Displacement Curve

After getting the deformed shape, we also obtain a value of displacement vertical, U3, then we can sketch the relation between applied force and displacement (Fig.17-20) for each wire mesh net configurations based from Fig.16.

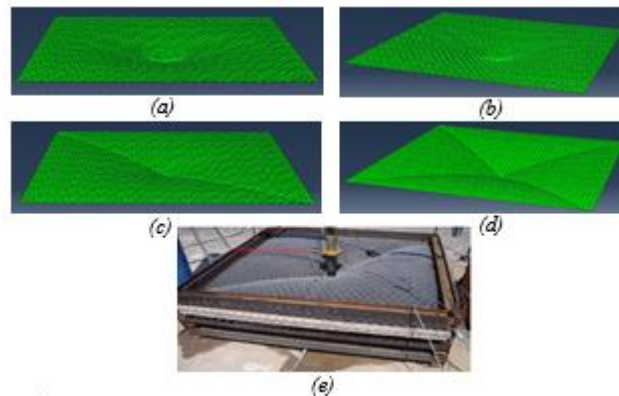


Figure.15. Deformed shape : (a) Wire mesh 60x80 , (b) Wire mesh 100x120, (c) Wire mesh with 1 cable, (d) Wire mesh with 2 cables, (e) Wire mesh with 2 cables (experiment).

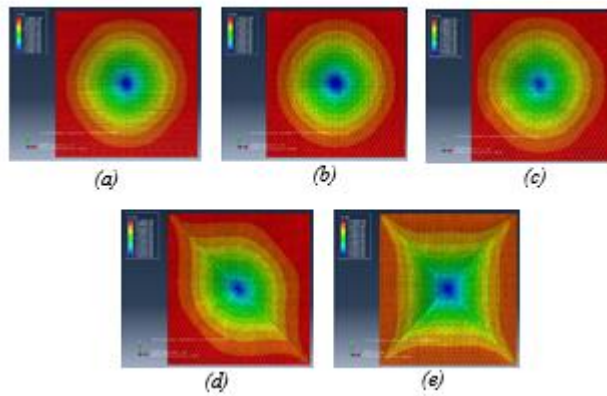


Figure.16. Displacement vertical, U_3 : (a) Wire mesh 60x80 , (b) Wire mesh 100x120, (c) Double sheet wire mesh, (d) Wire mesh with 1 cable, (e) Wire mesh with 2 cables.

TABLE V. Comparison of Displacement, U_3

Configuration	Displacement (cm)	
	Num.	Exp.
Wire mesh 60x80	27.8	26.8
Wire mesh 100x120	26.5	25.3
Double sheet wire mesh 100x120	30.2	33.4
Wire mesh with 1 cable	26.5	26.9
Wire mesh with 2 cables	34.1	34.2

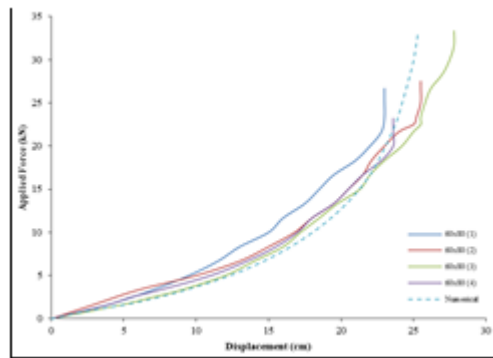


Figure.17. Comparison between experimental and numerical results of Wire mesh net 60x80

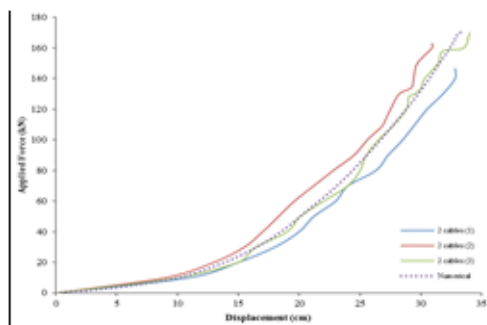


Figure.18. Comparison between experimental and numerical results of Wire mesh net 100x120 with 2 cables.

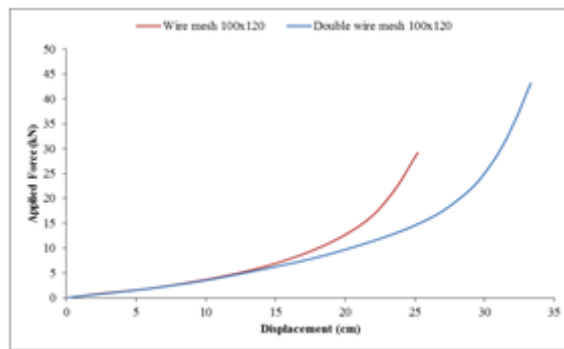


Figure.19. Numerical analysis comparison between single wire mesh 100x120 and double wire mesh 100x120.

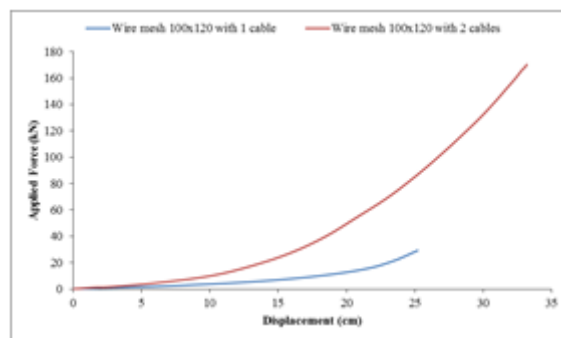


Figure.20. Numerical analysis comparison between wire mesh 100x120 with 1 cable and wire mesh 100x120 with 2 cables.

C. Stress Analysis

To find out what will happen to the structure of the net in the numerical modeling, we have observed stress that occurs on the wire. If the maximum stress obtained numerically exceeds the ultimate strength limit of the wire mesh net, then the structure collapses. Fig. 21 is a sketch of the area on the wire with maximum stress is shown in red color. Table 6 summarizes the stress in this related area.

D. Conclusion

The basic idea of any numerical method for differential equation is to discretize the continuous problem given with.

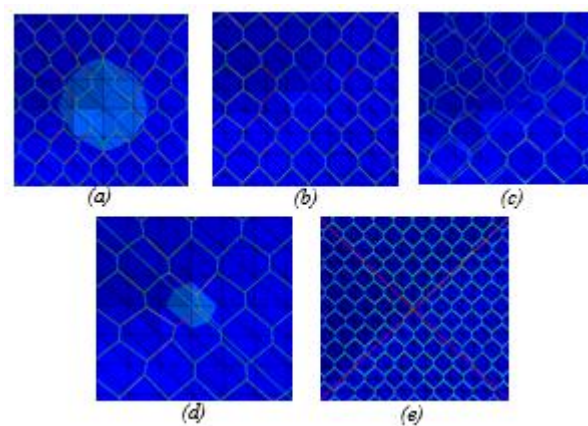


Figure.21. Location of maximal stress (in red color): (a) Wire mesh 60x80, (b) Wire mesh 100x120, (c) Double sheet wire mesh, (d) Wire mesh with 1 cable, (e) Wire mesh with 2 cables.

TABLE VI. Summary of maximum stress

Configuration	Ultimate Strength (N/mm ²)	Maximum Stress (N/mm ²)	Location of Maximum
Wire mesh 60x80	500 ^a	219	On net
Wire mesh 100x120	500 ^a	218	On net
Double sheet wire mesh 100x120	500 ^a	338	On net
Wire mesh with 1 cable	500 ^a	341	On net
Wire mesh with 2 cables	1300 ^b	572	On cable

^a: wire mesh net, ^b: cable

infinite degrees of freedom for a problem or a discrete equations that can be done only solved using a computer. Using quasi-static loading process is capable to respond the complex problems as results shown. After studying the behavior of wire mesh net configurations, we can not say that the results obtained experimentally and numerically stick perfectly. For example, in the part of experimental, there was a rupture, but in numerical analysis, we see that the system works in elastic condition. On the other hand, the result of curve of applied force versus displacement are close with the test.

REFERENCES

- [1]. A. Cazzani, L. Mongiovi, T. Frenez. Dynamic finite element analysis of interceptive devices for falling rocks. *Int. J. Rock. Lech. Min. Sci.* 2002;39(3):303-21.
- [2]. Trad, "Behavior analysis and modelling of the protected structures: case study wire mesh screen of rockfall under static and dynamic loadings", Lyon: INSA de Lyon, 2011.
- [3]. Volkwein, K. Schellenberg, V. Labiouse, F. Agliardi, F. Berger, F. Bourrier. Rockfall characterization and structural protection – a review. *Nat. Hazard Earth Syst. Sci.* 2011;11:2617-51.
- [4]. B. Muhunthan, S. Shu, N. Sasiharan, O.A. Hattamleh, T.C. Badger, S.M. Lowell. Analysis and design of wire mesh/cable net slope protection. Tech. rep., Washington State Transportation Center, Washington; 2005.
- [5]. Bertrand, F. Nicot, P. Gotteland, S. Lambert. Discrete element method (DEM) numerical modeling of double-twisted hexagonal mesh. *Canadian Geotech J.* 2008;45(8):1104-17.
- [6]. Jeannin, "Project study of wire mesh net anchored", Grenoble: Polytech de Grenoble, 2013.
- [7]. Nicot, B. Cambou, G. Mazzoleni. Design of rockfall restraining nets from a discrete element modeling. *Rock Lech. Rock Eng.* 2001;34:99-118.
- [8]. J.J. Del Coz Diaz, P.J. Garcia Nieto, F. Rodriguez Mazon, F.J. Suarez Dominguez, 2002 Design and finite element analysis of a wet cycle cement rotary kiln. *Finite elements in Analysis and Design* 39(1), 17-42.
- [9]. K. Thoeni, C. Lambert, A. Giacomini, S.W. Sloan. Discrete modelling of hexagonal wire meshes with a stochastically distorted contact model. *Comp. and Geotech. J.* 2013;49:158-169.
- [10]. O. Zienkiewicz, R. Taylor, *The Finite Element Method: Solid and Fluid Mechanics and Non-linearity.* London: McGraw-Hill Book Company, 1991.
- [11]. S. Brenner, L. Scott, *The Mathematical Theory of Finite Element Method.* Berlin: Springer-Verlag, 2002.
- [12]. S.R. Potula, K.N. Solanki, D.L. Oglesby. Investigating occupant safety through simulating the interaction between side curtain airbag deployment and an out-of-position occupant. *Int. J. Accident Analysis and Prevention.* 2012;49:392-403.

